AD-A070 458 NAVAL POSTGRADUATE SCHOOL MONTEREY CA F/G 4/2
USE OF GALERKIN METHODS IN NUMERICAL WEATHER PREDICTION.(U)
DEC 78 R T WILLIAMS
UNCLASSIFIED NPS63-78-006 NL

| OF |
AD A070458

END
DATE FILMED
7-79
DDC

NPS63-78-006

LEVEL

NAVAL POSTGRADUATE SCHOOL

Monterey, California

USE OF GALERKIN METHODS IN

NUMERICAL WEATHER PREDICTION

by

R. T. Williams

December 1978

Technical Report Period: October 1977-December 1978

Approved for public release; distribution unlimited.

Prepared for: Naval Environmental Prediction Research Facility
and Fleet Numerical Weather Central

NAVAL POSTGRADUATE SCHOOL
Monterey, California 93940

Rear Admiral Tyler F. Dedman
Superintendent

J. R. Borsting
Provost

The work reported herein was supported by the Naval Environmental Prediction Research Facility and the Fleet Numerical Weather Central.

This report was prepared by:

R. T. Williams

R. T. Williams
Professor of Meteorology

Reviewed by:

G. J. Haltiner

G. J. Haltiner, Chairman
Department of Meteorology

Released by:

William M. Tolles

W. M. Tolles
Dean of Research

Unclassified

SECURITY CLASSIFICATION OF THIS PAGE (When Data Entered)

REPORT DOCUMENTATION PAGE		READ INSTRUCTIONS BEFORE COMPLETING FORM
(14) 1. REPORT NUMBER NPS63-78-006	2. GOVT ACCESSION NO.	3. RECIPIENT'S CATALOG NUMBER
(6) 4. TITLE (and Subtitle) Use of Galerkin Methods in Numerical Weather Prediction.		TYPE OF REPORT & PERIOD COVERED Report for Oct 77 - Dec 1978
		6. PERFORMING ORG. REPORT NUMBER
(10) 7. AUTHOR(s) R. T. Williams		8. CONTRACT OR GRANT NUMBER(s)
9. PERFORMING ORGANIZATION NAME AND ADDRESS Naval Postgraduate School Monterey, California 93940	251 450	10. PROGRAM ELEMENT, PROJECT, TASK AREA & WORK UNIT NUMBERS N6685678WR78018 N63134-78-WR-80806
11. CONTROLLING OFFICE NAME AND ADDRESS Naval Environmental Prediction Research Facility and Fleet Numerical Weather Central Monterey, California 93940	(11)	12. REPORT DATE December 1978 13. NUMBER OF PAGES 53
14. MONITORING AGENCY NAME & ADDRESS(if different from Controlling Office) (12) 53 p.		15. SECURITY CLASS. (of this report) Unclassified
		15a. DECLASSIFICATION/DOWNGRADING SCHEDULE

16. DISTRIBUTION STATEMENT (of this Report)

Approved for public release; distribution unlimited.

17. DISTRIBUTION STATEMENT (of the abstract entered in Block 20, if different from Report)

(9) Technical Rept. Oct 77-Dec 78,

18. SUPPLEMENTARY NOTES

19. KEY WORDS (Continue on reverse side if necessary and identify by block number)

Finite Element Method
Spectral Method
Numerical Methods

20. ABSTRACT (Continue on reverse side if necessary and identify by block number)

In this report the Galerkin method is presented and the spectral and finite element methods are shown to be special cases of the general method. The spectral and finite element methods are applied to a simple linear equation and compared. The spectral method is then applied to the non-linear barotropic vorticity equation in Cartesian coordinates and in spherical coordinates. The transform technique is presented which allows efficient treatment of the nonlinear terms in the spectral method. This

DD FORM 1 JAN 73 1473 EDITION OF 1 NOV 65 IS OBSOLETE S/N 0102-014-6601

Unclassified 251 450

SECURITY CLASSIFICATION OF THIS PAGE (When Data Entered)

79 06 25 05

(cont)

method is also applied to the shallow water equations. The finite element method with linear basis functions is applied to the linear advection equation and compared to second and fourth order finite difference approximations. The nonlinear barotropic vorticity is also developed in finite elements.

A

TABLE OF CONTENTS

List of Figures

List of Tables

1. Introduction

Finite difference methods specify the dependent variables at certain grid points in space and time, and the derivatives in the equations are evaluated using Taylor series approximations. The Galerkin procedure, which will be treated in this chapter, represents the dependent variables with a sum of functions which have a prescribed spatial structure. The coefficient associated with each function is normally a function of time. This procedure transforms a partial differential equation into a set of ordinary differential equations for the coefficients. These equations are usually solved with finite differences in time. The two most useful Galerkin methods are the spectral method and the finite element method. The spectral method, which employs orthogonal functions, has been used in meteorological problems for a number of years. The finite element method employs functions which are zero except in a limited region where they are low order polynomials. This method, which was developed in engineering, has only recently been introduced into meteorology and oceanography.

The Galerkin procedure can be illustrated with the following equation:

$$\mathcal{L}(u) = f(x) \tag{1}$$

where $\mathcal{L}$ is a differential operator, u is the dependent variable and $f(x)$ is a specified forcing function. Suppose that (1) is to be solved in the domain $a \leq x \leq b$ and that appropriate boundary conditions are provided. Consider a series of linearly independent functions $\varphi_j(x)$ which will be called basis functions. The next step is to expand $u(x)$ into a series as follows:

$$u(x) = \sum_{j=1}^{N} u_j \varphi_j(x) , \tag{2}$$

where u_j is the coefficient for jth basis function. The error in satisfying the differential equation (1) with the N terms of the sum (2) is

$$e_N = \mathcal{L}\left(\sum_{j=1}^{N} u_j \varphi_j\right) - f(x) \ . \tag{3}$$

The Galerkin procedure requires that the error be orthogonal to each basis function in the following sense:

$$\int_a^b e_N \varphi_i dx = 0 \ , \quad i=1,\ldots,N \ . \tag{4}$$

The final form is obtained by substituting (3) into (4):

$$\int_a^b \varphi_i \mathcal{L}\left(\sum_{j=1}^{N} u_j \varphi_j\right) dx - \int_a^b \varphi_i f(x) dx = 0 \ , \quad i=1,\ldots,N \ . \tag{5}$$

This reduces the problem to N algebraic equations which relate the unknown coefficients u_j to the "transforms" of the forcing function. This procedure is quite general and can be applied to more dependent and independent variables.

2 Example with Spectral and Finite Element Methods

Now the spectral method and the finite element method will be applied to the following simple form of (1):

$$\frac{d^2u}{dx^2} = f(x) \ , \quad o \leq x \leq \pi \ . \tag{6}$$

The boundary conditions are

$$u(o) = u(\pi) = 0 \ . \tag{7}$$

For the spectral method the following basis functions are appropriate:

$$\varphi_j = \sin jx \ , \quad j=1,\ldots,N \ . \tag{8}$$

These functions are orthogonal on the interval $0 \le x \le \pi$ and they satisfy the boundary conditions (7). With these basis functions

$$\mathcal{L}\left(\sum_{j=1}^{N} (u_j\varphi_j)\right) = \sum_{j=1}^{N} (-j^2)u_j\varphi_j \ ,$$

and (5) becomes

$$-\sum_{j=1}^{N} j^2 u_j \int_0^{\pi} \varphi_i\varphi_j dx = \int_0^{\pi} \varphi_i f(x)dx \ , \quad i=1,\ldots,N. \tag{9}$$

The product of the basis functions can be written

$$\int_0^{\pi} \sin ix \sin jx \, dx = \frac{1}{2}\int_0^{\pi} [\cos(i-j)x-\cos(i+j)x]dx = (\pi/2)\delta_{ij} \ , \tag{10}$$

where δ_{ij} is the Kronecker delta which satisfies $\delta_{ij} = 1$ if $i = j$ and $\delta_{ij} = 0$ if $i \neq j$. Equation (10) is merely the orthogonality condition which arises since the integral vanishes except when $i = j$. With the use of (10), the solution to (9) becomes

$$u_i = -\frac{2}{\pi i^2}\int_0^{\pi} \varphi_i f \, dx \ . \tag{11}$$

Each coefficient is proportional to the finite Fourier transform of the forcing term. In this example both the error in the solution and the error in the differential equation are orthogonal to the basis functions. This is because $\mathcal{L}(\varphi_i)$ is proportional to φ_i so that if the error is orthogonal to $\mathcal{L}(\varphi_i)$ it will also be orthogonal to φ_i. This will also be true when certain other linear equations are treated with the spectral method, but it will not generally be true with nonlinear equations.

Now consider the same differential equation (6) with the finite element method. Divide the interval $0 \leq x \leq \pi$ into N+1 segments such that $(N+1)\,\Delta x = \pi$. The basis functions are chosen to be tent shaped piecewise linear functions which are also called chapeau functions, as shown in Figure 1. As can be seen from the

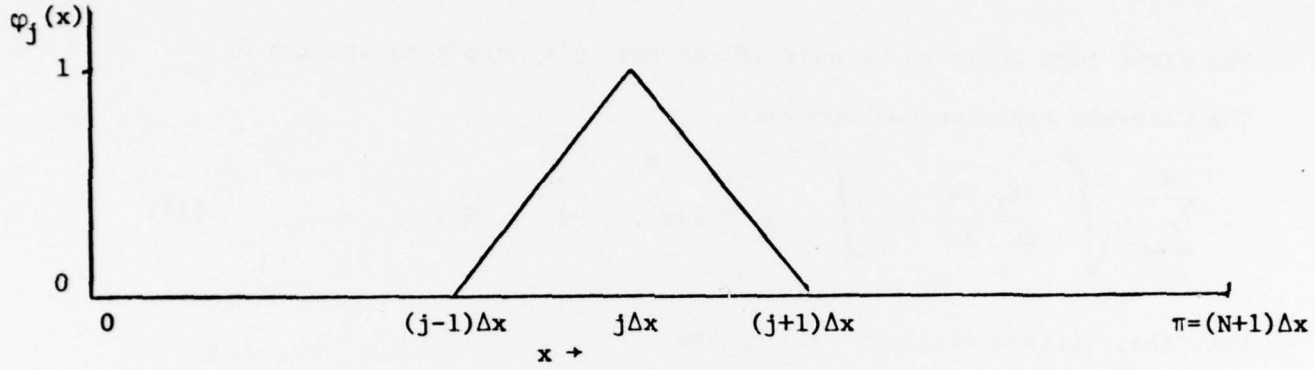

Fig. 1. Piecewise linear basis function.

Figure, $\varphi_j(x)$ has a maximum of 1 at $x = j\Delta x$, which is called the nodal point. The basis function decreases linearly to zero at $x = (j-1)\Delta x$, and it is zero everywhere else. Mathematically $\varphi_j(x)$ is defined as follows:

$$\varphi_j(x) = \left\{ \begin{array}{ll} 0\,, & x > (j+1)\Delta x \quad \text{or} \quad x < (j-1)\Delta x \\ (x-(j-1)\Delta x)/\Delta x\,, & (j-1)\Delta x \leq x \leq j\Delta x \\ ((j+1)\Delta x - x)/\Delta x\,, & j\Delta x \leq x \leq (j+1)\Delta x \end{array} \right\} \quad . \tag{12}$$

Note that the coefficient u_j is actually the value of the function at $x = j\Delta x$ since $\varphi_j(j\Delta x) = 1$ and $\varphi_i(j\Delta x) = 0$ for $i \neq j$. These elements are not quite orthogonal, but only adjacent elements interact. The boundary conditions (7) are automatically satisfied although this is not necessary in many cases with finite elements.

Equation (5) now becomes

$$\sum_{j=1}^{N} u_j \int_0^{\pi} \varphi_i \frac{d^2\varphi_j}{dx^2}\,dx - \int_0^{\pi} \varphi_i f(x)\,dx = 0 \,.$$

This form of the equation is not appropriate because it involves a second derivative of the basis function which is only piecewise linear. However, this problem can be avoided by integrating the first term by parts as follows:

$$\sum_{j=1}^{N} u_j \int_0^{\pi} \left[\frac{d}{dx}\left(\varphi_i \frac{d\varphi_j}{dx}\right) - \frac{d\varphi_i}{dx}\frac{d\varphi_j}{dx}\right]dx - \int_0^{\pi} \varphi_i f(x)dx = 0 .$$

The first term vanishes because all of the φ's are zero at $x = 0, \pi$.

The Galerkin equation now becomes

$$-\sum_{j=1}^{N} u_j \int_0^{\pi} \frac{d\varphi_i}{dx}\frac{d\varphi_j}{dx}dx = \int_0^{\pi} \varphi_i f(x)dx , \quad i=1,\ldots,N . \tag{13}$$

Note that differentiating (12) gives:

$$\frac{d\varphi_j}{dx} = \left\{ \begin{array}{ll} 0 & , x > (j+1)\Delta x \quad \text{or } x < (j-1)\Delta x \\ 1/\Delta x & , (j-1)\Delta x \le x \le j\Delta x \\ -1/\Delta x & , j\Delta x \le x \le (j+1)\Delta x \end{array} \right\} . \tag{14}$$

The left hand side of (13) is easily evaluated since only 3 terms in the sum are different from zero:

$$-\sum_{j=1}^{N} u_j \int_0^{\pi} \frac{d\varphi_i}{dx}\frac{d\varphi_j}{dx}dx = \frac{u_{i-1}\Delta x - 2u_i\Delta x + u_{i+1}\Delta x}{\Delta x^2} . \tag{15}$$

The right hand integral in (13) may be evaluated if $f(x)$ is approximated in terms of the basis functions:

$$f(x) = \sum_{j=1}^{N} f_j \varphi_j , \tag{16}$$

so that the integral becomes

$$\int_0^{\pi} \varphi_i f(x)dx = \sum_{j=1}^{N} f_j \int_0^{\pi} \varphi_i \varphi_j dx = \sum_{j=1}^{N} f_j \int_{(i-1)\Delta x}^{(i+1)\Delta x} \varphi_i \varphi_j dx .$$

If $\xi = x - i\Delta x$ is introduced the integral can be expanded into three integrals:

$$\int_0^{\pi} \varphi_i f(x)dx = -f_{i-1} \int_{-\Delta x}^{0} \frac{\xi(\xi+\Delta x)}{\Delta x^2} d\xi + 2f_i \int_{-\Delta x}^{0} \frac{(\xi+\Delta x)^2}{\Delta x^2} d\xi + f_{i+1} \int_0^{\Delta x} \frac{\xi(\Delta x-\xi)}{\Delta x^2} d\xi \ . \tag{17}$$

When these terms have been evaluated, (17) and (15) can be substituted into (13) which gives

$$\frac{u_{i+1} - 2u_i + u_{i-1}}{\Delta x^2} = \frac{f_{i+1} + 4f_i + f_{i-1}}{6} \ . \tag{18}$$

This equation applies for $2 \leq i \leq N-1$ and the equations for $i = 1$ and $i = N$ are obtained by removing any terms in $i = 0$ or $i = N+1$. Equation (18) may be solved by Gaussian elimination

Since each coefficient in this finite element expansion represents the solution at a certain point in space, it is convenient to compare (18) with finite difference forms of (6). The centered difference form (4) of this equation is

$$\frac{u_{i+1} - 2u_i + u_{i-1}}{\Delta x^2} = f_i \ , \tag{19}$$

where $u_i = u(i\Delta x)$. The finite element equation (18) and the finite difference equation (19) are the same, except that the forcing term in (18) appears in a weighted average. When these equations are solved with a $f(x)$, which is sinusoidal, the finite element form is considerably more accurate for the shorter wavelengths.

In this example it appears that the spectral method is superior because the solution error is actually orthogonal to the basis functions. This is

not generally true with the finite element method because $L(u_i)$ depends on u_{i-1}, u_i and u_{i+1}. Each increase in N will normally change all of the solutions u_i, whereas with the spectral method the original N amplitudes are not changed because they are already exact. However if the variation of f should require fine resolution in only a small area, the finite element method can easily be applied by letting Δx vary. In this case the spectral method would require more elements because its spatial resolution is uniform. It is also clear that the finite element method can be used to design better finite difference equations.

3 Time Dependence

In the previous sections the Galerkin procedure has been applied to one-dimensional equations which are independent of time. The treatment of time variation is important for most meteorological prediction problems. Consider the following simplified equation:

$$\frac{\partial u}{\partial t} + \mathcal{L}(u) = 0 \ , \tag{20}$$

where the operator $\mathcal{L}$ may be nonlinear. Expand $u(x,t)$ into a series as follows:

$$u(x,t) = \sum_{j=1}^{N} u_j(t)\varphi_j(x) \ , \tag{21}$$

where the coefficients $u_j(t)$ are functions of time and the basis functions $\varphi_j(x)$ are functions of x. Usually the Galerkin procedure is not applied to the time dependence because it is more convenient to ue finite differences in time.

The Galerkin form of (20) is obtained by substituting (21) into (20), multiplying by $\varphi_i(x)$ and integrating over the domain as follows:

$$\sum_{j=1}^{N} \frac{du_j}{dt} \int_a^b \varphi_i \varphi_j dx + \int_a^b \varphi_i \mathcal{L}(\Sigma u_j \varphi_j) dx = 0 , \quad i=1,\ldots,N . \tag{22}$$

This process gives N coupled ordinary differential equations in the coefficients $u_j(t)$. This set can be solved by introducing finite differences in time.

The importance of energy conserving finite difference schemes is well known. The Galerkin method leads naturally to energy conservation in equations with quadratic energy variants. To show this, multiply (20) by u and integrate with respect to x :

$$\int_a^b \frac{\partial(u^2/2)}{\partial t} dx = -\int_a^b u \mathcal{L}(u) dx . \tag{23}$$

For an energy conserving system, the operator must satisfy the condition

$$\int_a^b u \mathcal{L}(u) dx = 0 , \tag{24}$$

where u is any function which satisfies the boundary conditions. In this case (23) becomes

$$\frac{d}{dt} \int_a^b u^2/2 \, dx = 0 , \tag{25}$$

which shows the energy conservation for the exact equation. To demonstrate that the same result holds for the finite sum (21), multiply the ith equation of (22) by u_i and sum from i=1 to i=N :

$$\int_a^b (\sum_{i=1}^{N} u_i \varphi_i) \frac{\partial}{\partial t} (\sum_{j=1}^{N} u_j \varphi_j) dx = -\int_a^b (\sum_{i=1}^{N} u_i \varphi_i) \mathcal{L} (\sum_{j=1}^{N} u_j \varphi_j) . \tag{26}$$

The integral on the right vanishes from (24) since the function given by (21) satifies the boundary conditions. Therefore (26) can be written

$$\int_a^b \frac{\partial}{\partial t}\left(\sum_{i=1}^{N} u_i\varphi_i\right)^2/2 \, dx = 0 \, , \tag{27}$$

which expresses the energy conservation for the Galerkin approximation to the spatial variation. As with finite difference equations the actual degree of energy conservation will depend on the time differencing which is used in (22).

4 Barotropic Vorticity Equation with Fourier Basis Functions

In this section the spectral method will be applied to the barotropic vorticity equation on the beta plane. Fourier basis functions are appropriate for the beta plane when the fields are periodic in x and y. The development of this section closely follows Lorenz (1960). The barotropic vorticity equation may be written:

$$\frac{\partial}{\partial t}\nabla^2\psi + \vec{k} \times \nabla\psi \cdot \nabla(\nabla^2\psi) + \beta \, \partial\psi/\partial x = 0 \, , \tag{28}$$

where ψ is the streamfunction. Suppose that the fields are periodic in both x and y so that

$$\psi(x + 2\pi/k, y + 2\pi/\ell, t) = \psi(x,y,t) \, . \tag{29}$$

With the beta plane geometry and the periodicity condition, the appropriate orthogonal basis functions are of the form:

$$\varphi_{mn}(x,y) = e^{i(mkx+n\ell y)} \, . \tag{30}$$

These functions are eigensolutions of the equation:

$$\nabla^2\varphi + b\varphi = 0 \tag{31}$$

where the eigenvalues are given by

$$b = (m^2k^2 + n^2\ell^2) \ . \tag{32}$$

The streamfunction can be expanded in terms of this basis functions as follows:

$$\psi(x,y,t) = \sum_{m} \sum_{n} C_{mn}(t)\ e^{i(mkx+n\ell y)} \ .$$

In order for ψ to be real the coefficients must satisfy the condition

$$C_{mn} = C^{*}_{-m-n} \ ,$$

where $(\ )^{*}$ indicates the complex conjugation. This can be shown by considering only the m,n and $-m,-n$. It is convenient to introduce the wave number vector $\vec{M} = mk\vec{i} + n\ell\vec{j}$ and the radius vector $\vec{R} = x\vec{i} + y\vec{j}$. The expansion for ψ can now be written

$$\psi(x,y,t) = \sum_{\vec{M}} C_{\vec{M}}(t)\ e^{i\vec{M}\cdot\vec{R}} \ . \tag{33}$$

With the use of (31) and (33) the vorticity can be written

$$\nabla^2\psi = -\sum_{\vec{M}} (\vec{M}\cdot\vec{M})\ C_{\vec{M}}(t)\ e^{i\vec{M}\cdot\vec{R}} \ . \tag{34}$$

The quantities which are required in the nonlinear term in (28) may be written:

$$\nabla\psi = \sum_{\vec{H}} i\vec{H}\ C_{\vec{H}}\ e^{i\vec{H}\cdot\vec{R}}$$

$$\nabla(\nabla^2\psi) = -\sum_{\vec{L}} i\vec{L}(\vec{L}\cdot\vec{L})\ C_{\vec{L}}\ e^{i\vec{L}\cdot\vec{R}} \ . \tag{35}$$

The wavenumber vectors $\vec{H}$ and $\vec{L}$ are introduced because the sums must be multiplied together and rearranged.

Now substitute the various sums [(33), (34) and (35)] into (28) which gives:

$$-\sum_{\vec{L}} (\vec{L}\cdot\vec{L})\frac{d}{dt} C_{\vec{L}}\, e^{i\vec{L}\cdot\vec{R}} + \sum_{\vec{L}}\sum_{\vec{H}} (\vec{L}\cdot\vec{L})\vec{k}\cdot\vec{H}\times\vec{L}\; C_{\vec{H}}C_{\vec{L}}\, e^{i(\vec{H}+\vec{L})\cdot\vec{R}}$$

$$+ im\beta k\sum_{\vec{L}} C_{\vec{L}}\, e^{i\vec{L}\cdot\vec{R}} = 0 . \qquad (36)$$

The Galerkin method for this equation is similar to the method used in (22), except that the equation must be multiplied by the complex conjugate of the basis function since the basis function is complex. To carry out this process multiply (36) by $e^{-i\vec{M}\cdot\vec{R}}$ and integrate over the periodic domain as follows:

$$\int_0^{2\pi/k}\int_0^{2\pi/\ell} \left\{ -\sum_{\vec{L}} (\vec{L}\cdot\vec{L})\, \frac{d}{dt} C_{\vec{L}}\, e^{i(\vec{L}-\vec{M})\cdot\vec{R}} + im\beta k\sum_{\vec{L}} C_{\vec{L}}\, e^{i(\vec{L}-\vec{M})\cdot\vec{R}} \right.$$

$$\left. + \sum_{\vec{L}}\sum_{\vec{H}} (\vec{L}\cdot\vec{L})\vec{k}\cdot\vec{H}\times\vec{L}\; C_{\vec{H}}C_{\vec{L}}\, e^{i(\vec{H}+\vec{L}-\vec{M})\cdot\vec{R}} \right\} dydx = 0 ,$$

for each $\vec{M}$ in the original sum (33). Each integral of the exponential function will vanish except when the exponent is zero. This leads to the following equation for each $\vec{M}$:

$$\frac{dC_{\vec{M}}}{dt} + \frac{im\beta k C_{\vec{M}}}{\vec{M}\cdot\vec{M}} + \sum_{\vec{H}} \frac{(\vec{M}-\vec{H})\cdot(\vec{M}-\vec{H})\vec{k}\cdot\vec{H}\times\vec{M}}{\vec{M}\cdot\vec{M}}\, C_{\vec{M}-\vec{H}}\, C_{\vec{H}} = 0 . \qquad (37)$$

In the first two terms the contribution occurs for $\vec{L} = \vec{M}$ and in the last term for $\vec{L} = \vec{M} - \vec{H}$.

Equation (3) represents N ordinary differential equations, where N is the number of terms in the sum (33). The last term in the equation gives the interaction between different waves which comes from the nonlinear advection term in (28). In particular wave $\vec{M}$ is affected by the interaction of waves $\vec{H}$ and $\vec{M} - \vec{H}$. When the last term is dropped, (3) becomes a set of linear, uncoupled equations which can be solved to give the Rossby wave solution.

In section (3) it was pointed out that the Galerkin procedure preserves energy type univariants which arise from quadratic nonlinearities in the original equations. Equation (28) conserves both kinetic energy and mean square vorticity or enstrophy. The kinetic energy for the region can be written:

$$K = \int_0^{2\pi/k} \int_0^{2\pi/\ell} \frac{\nabla\psi \cdot \nabla\psi}{2} \, dydx = \frac{1}{2} \sum_{\vec{H}} \sum_{\vec{M}} i^2 \, \vec{H} \cdot \vec{M} C_{\vec{H}} C_{\vec{M}} \int_0^{2\pi/k} \int_0^{2\pi/\ell} e^{i(\vec{H}+\vec{M}) \cdot \vec{R}} \, dydx \, ,$$

where the $\nabla\psi$ product was obtained from (35) with different summations. The integral on the right is nonzero only when $\vec{H} = -\vec{M}$ so that the energy can be written

$$K = \frac{1}{2} \sum_{\vec{M}} \vec{M} \cdot \vec{M} C_{\vec{M}} C_{-\vec{M}} = \frac{1}{2} \sum_{\vec{M}} \vec{M} \cdot \vec{M} |C_{\vec{M}}|^2 \, , \qquad (38)$$

where the condition $C_{-\vec{M}} = C^*_{\vec{M}}$ has been used in the last step.

The energy form in (38) is conserved ($dK/dt = 0$) by both the original vorticity equation (28) and the spectral form (37). The conservation for (28) is easily demonstrated, and the conservation for (38) follows

from the development in section (3). An equation for the rate of change of energy in wave $\vec{M}$ can be obtained by differentiating $C_{\vec{M}}C_{-\vec{M}}$ with respect to t and by using (37). The resulting equation shows that the energy in wave $\vec{M}$ changes in proportion $C_{\vec{M}}$ times the amplitudes of pairs of interacting waves. Thus if $C_{\vec{M}}$ is maintained at zero, the energy flow out of the other waves to it must be zero. This shows in another way that energy will be conserved in any set of waves that might be selected for sum (33). Since interactions outside of this set are neglected, aliasing cannot occur in a spectral model. This automatically eliminates the nonlinear computational instability which occurs with finite difference equations.

The set of ordinary differential equations (37) can be integrated numerically with one of the standard schemes. In fact Baer and Platzman (1961) noted that the linear terms in (37) can be treated exactly so that the only time differencing errors comes from the nonlinear terms.

It is clear that the spectral method is much more accurate than most finite difference methods for the same number of degrees of freedom. In particular, linear advection that was examined is treated exactly by the spectral method provided that the initial field in resolved. Finite difference methods experience false dispersion since the short waves move too slowly. The spectral method has no aliasing because interactions involving shorter waves outside of the truncated set are excluded. On the other hand, the finite differencing falsely reflects interactions with shorter waves back onto longer waves. With the Arakawa Jacobian finite difference forms, this aliasing does not produce spurious energy, but it does cause phase errors in the interacting waves. In spectral models the most important error involves the neglect of interactions with wave components which are outside of the original set. The neglect of these interactions

causes an error in the waves which are represented by the basis functions. Thus although the error in the original equation is orthogonal to the basis functions, the error in the solution will occur in the scales described by the basis functions.

When the spectral method is applied to a vorticity equation such as (28), a Poisson equation for $\partial\psi/\partial t$ does not have to be solved since the basis functions are eigensolutions of (31). The Poisson equation must be solved at each time step with finite difference methods. The biggest drawback to this form of the spectral equations is in calculating the nonlinear term which appears as the sum in (37). The coefficient preceding $C_{M-H}^{\rightarrow} C_{H}^{\rightarrow}$ is called the interaction coefficient and it is usually computed just once and stored for use during the integration of the equation. The problem is that if there are N degrees of freedom the number of operations needed to compute the nonlinear terms goes as N^2 for this spectral model as compared with N for most finite difference methods. Thus for high resolution (large N), this form of the spectral method requires relatively larger computer time than finite difference methods. In a later section a method which avoids this problem will be presented. However the present method is very convenient for low-order models. Lorenz (1960) obtained some very interesting nonlinear solutions with a 3-component system. It can be seen from (37) that at least 3 waves are required for nonlinear interaction.

5 Barotropic Vorticity Equation with Spherical Harmonics

In this section the spectral equations will be formulated for barotropic motion on the sphere. The barotropic vorticity equation in spherical coordinates can be written:

$$\frac{\partial}{\partial t}\nabla^2\psi - \frac{1}{a^2}\left[\frac{\partial\psi}{\partial\mu}\frac{\partial\nabla^2\psi}{\partial\lambda} - \frac{\partial\psi}{\partial\lambda}\frac{\partial\nabla^2\psi}{\partial\mu}\right] + \frac{2\Omega}{a^2}\frac{\partial\psi}{\partial\lambda} = 0 \ , \qquad (39)$$

where

$$\nabla^2 = \frac{\partial}{\partial\mu}[(1-\mu^2)\ \frac{\partial}{\partial\mu}] + \frac{1}{1-\mu^2}\ \frac{\partial^2}{\partial\lambda^2}\ . \tag{40}$$

In these equations λ is the longitude and $\mu = \sin\varphi$, where φ is the latitude. The spectral method was first applied in spherical coordinates by Silberman (1954) and the development of this section follows Platzman (1960).

The appropriate orthogonal basis functions are

$$Y_{m,n}\ (\mu,\ \lambda) = P_{m,n}(\mu)\ e^{im\lambda}\ , \tag{41}$$

where $P_{m,n}$ denotes associated Legendre functions of the first kind which are defined by

$$P_{m,n}(\mu) = [\frac{(2n+1)(n-m)!}{(n+m)!}]^{1/2}\ \frac{(1-\mu^2)^{m/2}}{2^n\ n!}\ \frac{d^{n+m}}{d\mu^{n+m}}\ (\mu^2-1)^n\ . \tag{42}$$

These basis functions are spherical harmonics which satisfy the equation

$$\nabla^2\ Y_{m,n} + b\ Y_{m,n} = 0\ , \tag{43}$$

where the eigenvalues are given by

$$b = n(n+1)/a^2\ . \tag{44}$$

Here $|m|$ is the planetary wave number and $n-|m|$ is the number of zeros between the poles. Also n must be greater than or equal to $|m|$. These basis functions are orthogonal so that

$$\frac{1}{4\pi}\int_0^{2\pi}\int_{-1}^{1} Y_{m,n}\ Y^*_{m',n'}\ d\mu d\lambda = \begin{cases} 1 & \text{for } (m',n') = (m,n) \\ 0 & \text{for } (m',n') \neq (m,n) \end{cases}\ . \tag{45}$$

The streamfunction can be expanded as follows:

$$\psi(x,y,t) = a^2 \sum_{m=-M}^{M} \sum_{n=|m|}^{|m|+J} \psi_{m,n}(t)\, Y_{m,n}(\lambda,\mu) \ . \qquad (46)$$

Since ψ must be real $\psi_{m,n}$ must satisfy

$$\psi_{-m,n} = (-1)^m \psi^*_{m,n} \ . \qquad (47)$$

This condition was derived with the use of the relation $P_{-m,n} = (-1)^m P_{m,n}$. The coefficients $\psi_{m,n}$ can be obtained from the inverse transform:

$$\psi_{n,m}(t) = \frac{1}{4\pi a^2} \int_0^{2\pi} \int_{-1}^{1} \psi(\lambda,\mu,t)\, Y^*_{m,n}\, d\mu d\lambda \ . \qquad (48)$$

The vorticity has the following expansion:

$$\nabla^2\psi = -\sum_{m=-M}^{M} \sum_{n=|m|}^{|m|+J} n(n+1)\ \psi_{m,n}(t)\, Y_{m,n} \ , \qquad (49)$$

which follows from (43) and (44).

The Galerkin method is applied by substituting (48) and (49) into (39), multiplying by $Y^*_{m,n}$ and integrating with respect to μ and λ . When the conditions (45) are employed this equation reduces to:

$$\frac{d\psi_{m,n}}{dt} = \frac{2\Omega m i}{n(n+1)}\, \psi_{m,n} - \frac{1}{n(n+1)}\, F_{m,n} \ . \qquad (50)$$

The nonlinear terms $F_{m,n}$ may be written

$$F_{m,n} = - \sum_{m_1=-M}^{M} \sum_{n_1=|m_1|}^{|m|+J} \sum_{m_2=-M}^{M} \sum_{n_2=|m_2|}^{|m_2|+J} i\psi_{m_1,n_1}\psi_{m_2,n_2}\, L(m,n;m_1,n_1;m_2,n_2) \ , \qquad (51)$$

where the interaction coefficients are given by

$$L(m,n;m_1,n_1;m_2,n_2) = \begin{cases} \frac{1}{2}[n_1(n_1+1)-n_2(n_2+1)]\int_{-1}^{1} P_{m,n}\{m_1 P_{m_1,n_1}\frac{dP_{m_2,n_2}}{d\mu} \\ \quad - m_2 P_{m_2,n_2}\frac{dP_{m_1,n_1}}{d\mu}\}d\mu \quad \text{for } m = m_1 + m_2 \\ = 0 \qquad\qquad \text{for } m \neq m_1 + m_2 \end{cases} . \tag{52}$$

In obtaining this result the subscripts 1 and 2 were used for expansions (48) and (49), respectively. This form for the interaction coefficients comes from the fact that $F_{m,n}$ changes sign when ψ_{m_1,n_1} and ψ_{m_2,n_2} are interchanged.

Equation (50) has the same form as the prediction equation (37) for the Fourier basis function. However the spherical coordinate equation has more complicated interaction coefficients because of the integral involving the Legendre functions. It can be shown by the same method as before that energy is conserved, and Platzman (1960) has also shown that mean square vorticity is conserved. The spectral method applied to spherical (global) prediction has the advantage that there are no singular points whereas singular points often cause problems with finite difference models. The only major disadvantage in solving (50) is in the large number of terms which come from the nonlinear terms. This problem will be treated in the next section.

6. Transform Method

In this section a new method for handling the nonlinear terms in (50) will be presented which avoids the use of interaction coefficients (see (51) and (52)). This method was formulated independently by Orszag (1970) and Eliasen, Machenhauer and Rasmussen (1970), and it has been reviewed by Bourke, McAvaney, Puri and Thurling (1977). The problem with the interaction coefficient method for computing nonlinear terms is that it requires multiplication of two series (together) which is very time consuming. The transform method sums the series at certain spatial grid points and these fields are multiplied together at each point to form the nonlinear terms. Then the nonlinear terms must be transformed back to spectral space. The usefulness of this process is enhanced by the existence of efficient transform methods. In spherical coordinates the fast Fourier transform is used in longitude and the Legendre integrals in latitude are evaluated by Gaussian quadrature. This method is far superior to the interaction coefficient method for the sphere.

The nonlinear terms which must be transformed may be rewritten as follows:

$$F(\mu,\lambda) = \frac{1}{a^2}\left[\frac{\partial\psi}{\partial\mu}\frac{\partial\nabla^2\psi}{\partial\lambda} - \frac{\partial\psi}{\partial\lambda}\frac{\partial\nabla^2\psi}{\partial\mu}\right] = \frac{1}{a^2}\left[\frac{\partial}{\partial\lambda}\left(\frac{\partial\psi}{\partial\mu}\nabla^2\psi\right) - \frac{\partial}{\partial\mu}\left(\frac{\partial\psi}{\partial\lambda}\nabla^2\psi\right)\right] . \tag{53}$$

It is now convenient to define the following quantities which are the λ and φ velocity components multiplied by $\cos\varphi$:

$$U \equiv \frac{-\cos^2\varphi}{a}\frac{\partial\psi}{\partial\mu} , \quad V \equiv \frac{1}{a}\frac{\partial\psi}{\partial\lambda} . \tag{54}$$

When these velocities are introduced into (53) it can be written as follows:

$$F(\mu,\lambda) = -\frac{1}{a}\left[\frac{1}{1-\mu^2}\frac{\partial}{\partial\lambda}(U\nabla^2\psi) + \frac{\partial}{\partial\mu}(V\nabla^2\psi)\right] . \tag{55}$$

The velocity components (54) can be computed from (46) at longitude-latitude grid points, and the vorticity can be obtained at the same points using 49). The details of the process will be given later. The products $U\nabla^2\psi$ and $V\nabla^2\psi$ can be calculated at each grid point and the resulting products can be Fourier analyzed in λ to give the following relations:

$$U\nabla^2\psi = a \sum_{m=-M}^{m=M} A_m(\mu)\, e^{im\lambda} ,$$
$$V\nabla^2\psi = a \sum_{m=-M}^{m=M} B_m(\mu)\, e^{im\lambda} . \qquad (56)$$

The transform of $F(\mu,\lambda)$ is given by

$$F_{m,n} = \frac{1}{4\pi} \int_0^{2\pi} \int_{-1}^{1} e^{-im\lambda} P_{m,n} F(\mu,\lambda)\, d\mu d\lambda . \qquad (57)$$

The λ integration in (57) can be carried out by substituting (56) into (55) and by inserting the result in (57), which gives:

$$F_{m,n} = -\frac{1}{2} \int_{-1}^{1} \left[\frac{im}{1-\mu^2} A_m P_{m,n} + \frac{dB_m}{d\mu} P_{m,n}\right] d\mu .$$

The second term can be integrated by parts which gives

$$F_{m,n} = -\frac{1}{2} \int_{-1}^{1} \left[\frac{im}{1-\mu^2} A_m P_{m,n} - B_m \frac{dP_{m,n}}{d\mu}\right] d\mu , \qquad (58)$$

where the condition $B_m = 0$ at $\mu = \pm 1$ was used to simplify the integral. This condition follows since V is equal to the actual velocity times $\cos\varphi$. The form of $F_{m,n}$ given by (58) is superior to the earlier form because only the known function $P_{m,n}$ is differentiated.

The integrand in (58) is a polynomial in μ and the integral can be evaluated following Eliasen et al. (1970) by the Gaussian quadrature formula. If the integrand is denoted by $Q(\mu)$, the formula gives the following expression for $F_{m,n}$:

$$F_{m,n} = \frac{1}{2} \sum_{k=1}^{K} G_k^{(K)} Q(\mu_k) . \qquad (59)$$

In (59) the summation is carried over K values of μ_k, where the μ_k's are roots of the Legendre polynomial $P_{0,K}$ and $G_k^{(K)}$ are the corresponding Gauss coefficients. The formula is exact for any polynomial of degree smaller than or equal to 2K-1 (see). Thus apart from roundoff errors, no approximation is introduced by computing the integral when a sufficiently high value of K is used. The maximum degree of $Q(\mu)$ can be most easily obtained from (52).

Before discussing this process for treating the nonlinear terms in more detail, it is necessary to determine the relation between J and M which must be defined in the sum (46). In rhomboidal truncation $J = M$, so that each latitudinal mode has the same number of waves in longitude. With triangular truncation $J = M - |m|$ so all basis functions which have the same scale $n(n+1)/a^2$, are either retained or dropped. Thus the mode with the smallest latitudinal scale has the largest longitudinal scale. Most meteorological models use the rhomboidal truncation in part because it gives better longitudinal resolution. In the remainder of this development, the rhomboidal truncation will be used.

In order to construct the fields (56) it is necessary to obtain U and V from ψ. First expand U and V into these sums:

$$U = \frac{1}{a} \sum_{m=-M}^{M} \sum_{n=|m|}^{|m|+M+1} U_{m,n} Y_{m,n} ,$$

$$V = \frac{1}{a} \sum_{m=-M}^{M} \sum_{n=|m|}^{|m|+M} V_{m,n} Y_{m,n} . \tag{60}$$

The following relations will be useful in evaluating (54):

$$(\mu^2-1) \frac{\partial Y_{m,n}}{\partial \mu} = n D_{m,n+1} Y_{m,n+1} - (n+1) D_{m,n} Y_{m,n-1} ,$$

$$\frac{\partial Y_{m,n}}{\partial \lambda} = im Y_{m,n} , \tag{61}$$

where $D_{m,n} \equiv [(n^2-m^2)/(4n^2-1)]^{\frac{1}{2}}$. The final expressions for $U_{m,n}$ and $V_{m,n}$ can be obtained by substituting (46) and (60) into (54), using (61) and by applying the orthogonality condition (45):

$$U_{m,n} = (n-1) D_{m,n} \psi_{m,n-1} - (n+2) D_{m,n+1} \psi_{m,n+1} ,$$

$$V_{m,n} = im \psi_{m,n} . \tag{62}$$

Note that the expansion for U as given in (60) must extend one degree above that defined for ψ, since nonzero values of $U_{|m|,|m|+M+1}$ are implied by nonzero values of $\psi_{|m|,|m|+M}$.

The quantities U, V and $\nabla^2\psi$ can now be evaluated at points

$$\lambda_j = 2\pi j/N , \quad \varphi_k = \arcsin \mu_k$$

where $j = 1, \ldots, N$ and $k = 1, \ldots, K$. The φ_k's are called the Gaussian latitudes. Consider for example $V(\lambda_j, \mu_k)$ which can be written:

$$V(\lambda_j, \mu_k) = \sum_{m=-M}^{M} e^{im\lambda_j} \left[\sum_{n=|m|}^{|m|+M} im\, \psi_{m,n}\, P_{m,n}(\mu_k) \right] , \qquad (63)$$

with the use of (41), (46) and (62). Similar expressions can be written for $U(\lambda_j, \mu_k)$ and $\nabla^2\psi(\lambda_j, \mu_k)$. The outer summation can be carried out very efficiently with the use of the fast Fourier transform method which was developed by Cooley and Tukey (1965). The number of operations required for the fast Fourier method applied over N points is of order $N \log_2 N$, while for the direct method order N^2 operations are required. The fast Fourier transform method is clearly much faster than the direct method for larger values of N. The next step is to compute $U\nabla^2\psi$ and $V\nabla^2\psi$ at each grid point. After these products have been computed, the Fourier transforms must be calculated to give A_m and B_m for use in (56). For example, using the discrete Fourier transform:

$$A_m(\mu_k) = \frac{1}{aN} \sum_{j=1}^{N} e^{-im\lambda_j} (U\nabla^2\psi)_{jk} , \qquad (64)$$

where $-M \leq m \leq M$. A similar expression is obtained for $B_m(\mu_k)$. The fast Fourier transform can also be used here to save time.

It is important to choose N large enough to avoid aliasing when the products are transformed back to wave number space as in equation (64). Orszag (1969), (1970) suggested that $N = 4M$ would be needed, but later Orszag (1971) and Machehauer and Rasmussen (1972) showed that $N = 3M+1$ was adequate to provide alias-free transforms.

Now that $A_m(\mu_k)$ and $B_m(\mu_k)$ are known, $F_{m,n}$ can be computed exactly from (59) if the degree of the polynomials is less than or equal to 2K-1. The maximum degree can be determined from (52) by noting that $P_{m,n}$ is a polynomial of degree n and by considering these selection rules for the interactions: $m = m_1 + m_2$, $|\ell_1 - \ell_2| < \ell < |\ell_1 + \ell_2|$. The conclusion which is given in Bourke et al. (1977) is that the maximum degree is 5M-1, so that the number of Gaussian latitudes is $K \geq 5\ M/2$.

This method of computing $F_{m,n}$ is more efficient than the interaction coefficient method and it requires much less computer storage. The number of calculations required for the interaction coefficient method is of order (M^5) while for the transform method it is of order $(25\ M^3)$ [see Bourke et al. (1977)]. It will be shown in the next section that the transform method is more efficient for even a moderate value of M and this advantage increases rapidly with M .

7 Spectral Model of Shallow Water Equations

In this section the spectral method will be extended to the primitive equations and it will be demonstrated that semi-implicit differencing can be applied with little extra effort. The shallow water equations in spherical coordinates will be used to demonstrate the procedure following Eliasen et al. (1970) and Bourke (1972). The equation of motion and the continuity equation can be written:

$$\frac{\partial \vec{V}}{\partial t} = -(\zeta+f)\ \vec{k} \times \vec{V} - \nabla(\phi' + \frac{\vec{V}\cdot\vec{V}}{2}) \ , \tag{65}$$

$$\frac{\partial \phi'}{\partial t} = -\nabla\cdot\phi'\vec{V} - \bar{\phi}\delta \ . \tag{66}$$

This form of the equation of motion will simplify the derivation of the vorticity and divergence equations. Note that the geopotential has been split into a mean $\bar{\phi}$, and a departure ϕ' , which will facilitate the implementation of semi-implicit time differencing.

The velocity is broken into rotational and divergent parts as follows:

$$\vec{V} = \vec{k} \times \nabla\psi + \nabla\chi = (U/\cos\varphi)\,\vec{i} + (V/\cos\varphi)\,\vec{j} \ . \tag{67}$$

The modified components U and V will also be used here. Now form the vorticity and divergence equations by taking $\nabla\cdot$ and $\vec{k}\cdot\nabla\times$ of (65) which gives:

$$\frac{\partial\zeta}{\partial t} = -\nabla\cdot(\zeta+f)\,\vec{V} \ , \tag{68}$$

$$\frac{\partial\delta}{\partial t} = \vec{k}\cdot\nabla\times[(\zeta+f)\,\vec{V}] - \nabla^2(\phi' + \frac{\vec{V}\cdot\vec{V}}{2}) \ . \tag{69}$$

The vorticity and divergence become

$$\zeta = \nabla^2\psi \ , \quad \delta = \nabla^2\chi \ . \tag{70}$$

In spectral models it is convenient to replace the equation of motion by the vorticity and divergence equations because the relations (70) are simplified when spherical harmonics are used as basis functions. This form of the equations is also more convenient for application of semi-implicit differencing.

The vorticity equation (68) and the divergence equation (69) can now be expanded with the use of (67) and (70) to give:

$$\frac{\partial}{\partial t}\nabla^2\psi = -\frac{1}{a\cos^2\varphi}\left[\frac{\partial}{\partial\lambda}(U\nabla^2\psi) + \cos\varphi\frac{\partial}{\partial\varphi}(V\nabla^2\psi)\right] - 2\Omega(\sin\varphi\,\nabla^2\chi + V/a) \ , \tag{71}$$

$$\frac{\partial}{\partial t}\nabla^2\chi = \frac{1}{a\cos^2\varphi}\left[\frac{\partial}{\partial\lambda}(V\nabla^2\psi) - \cos\varphi\frac{\partial}{\partial\varphi}(U\nabla^2\psi)\right] + 2\Omega(\sin\varphi\nabla^2\psi - U/a) - \nabla^2\left(\frac{U^2+V^2}{2\cos^2\varphi} + \phi'\right) \ . \tag{72}$$

Similarly the continuity equation (66) becomes:

$$\frac{\partial \phi'}{\partial t} = -\frac{1}{a \cos^2\varphi}\left[\frac{\partial}{\partial \lambda}(U\phi') + \cos\varphi \frac{\partial}{\partial \varphi}(V\phi')\right] - \bar{\phi}\nabla^2\chi \ . \tag{73}$$

The two components of (67) can be written:

$$U = -\frac{\cos\varphi}{a}\frac{\partial \psi}{\partial \varphi} + \frac{1}{a}\frac{\partial \chi}{\partial \lambda} \ , \tag{74}$$

$$V = \frac{1}{a}\frac{\partial \psi}{\partial \lambda} + \frac{\cos\varphi}{a}\frac{\partial \chi}{\partial \varphi} \ . \tag{75}$$

Equations (71), (72) and (73) are the predictive equations for ψ, χ and ϕ' and (74) and (75) are diagnostic expressions for U and V. The nonlinear terms in these equations are in a convenient form for the transform method which was presented in the last section, since the multiplication can be performed at the grid points before differentiation.

Each of the dependent variables is expanded in terms of the spherical harmonic basis functions (41) as follows:

$$\psi = a^2 \sum_{m=-M}^{M} \sum_{n=|m|}^{|m|+M} \psi_{m,n} Y_{m,n} \ , \quad \chi = a^2 \sum_{m=-M}^{M} \sum_{n=|m|}^{|m|+M} \chi_{m,n} Y_{m,n} \ , \tag{76}$$

$$\phi' = a^2 \sum_{m=-M}^{M} \sum^{|m|+M} \phi_{m,n} Y_{m,n} \ , \tag{77}$$

$$U = a \sum_{m=-M}^{M} \sum_{n=|m|}^{|m|+M+1} U_{m,n} Y_{m,n} \ , \quad V = a \sum_{m=-M}^{M} \sum_{n=|m|}^{|m|+M+1} V_{m,n} Y_{m,n} \ . \tag{78}$$

These expansions are for the rhomboidal wave number truncation. Equations (74) and (75) are transformed in the same manner as equations (54) were

in the last section and the result is

$$U_{m,n} = (n-1)D_{m,n}\psi_{m,n-1} - (n+2)D_{m,n+1}\psi_{m,n+1} + im\chi_{m,n} ,$$

$$V_{m,n} = -(n-1)D_{m,n}\chi_{m,n-1} + (n+2)D_{m,n+1}\chi_{m,n+1} + im\psi_{m,n} . \tag{79}$$

Note that the expansions for U and V must extend one degree above the expansions for ψ and χ.

The quantities needed for the nonlinear terms are obtained by evaluating the sums in (76), (77) and (78) at equally spaced points in longitude and at Gaussian latitudes. The required products are computed at each point and the products are then Fourier transformed in longitude as follows:

$$U\nabla^2\psi = a\sum_{m=-M}^{M} A_m e^{im\lambda} , \quad V\nabla^2\psi = a\sum_{m=-M}^{M} B_m e^{im\lambda} , \tag{80}$$

$$V\phi' = a^3\sum_{m=-M}^{M} C_m e^{im\lambda} , \quad V\phi' = a^3\sum_{m=-M}^{M} D_m e^{im\lambda} , \tag{81}$$

$$\frac{U^2 + V^2}{2} = a^2\sum_{m=-M}^{M} E_m e^{im\lambda} . \tag{82}$$

The spectral equations are formed by substituting (76), (77), (78), (80), (81) and (82) into the system (71)- (73) and multiplying each equation by $Y^*_{m,n}$ and integrating over the domain. With the use of the orthogonality condition (45) the equations finally reduce to the following set:

$$-n(n+1)\frac{\partial\psi_{m,n}}{\partial t} = \frac{1}{2}\int_{-1}^{1} \frac{1}{1-\mu^2}\left[imA_m P_{m,n} - B_m \frac{dP_{m,n}}{d\mu}\right] d\mu$$

$$+ 2\Omega[n(n-1)D_{m,n}\chi_{m,n-1} + (n+1)(n+2)D_{m,n+1}\chi_{m,n+1} - V_{m,n}] , \tag{83}$$

$$-n(n+1)\frac{\partial \chi_{m,n}}{\partial t} = \frac{1}{2}\int_{-1}^{1} \frac{1}{1-\mu^2}[imB_m P_{m,n} + A_m \frac{dP_{m,n}}{d\mu}]\, d\mu - 2\Omega[n(n-1)D_{m,n}\psi_{m,n-1}$$

$$+ (n+1)(n+2)D_{m,n+1}\psi_{m,n+1} + U_{m,n}] + n(n+1)(E_{m,n} + \phi_{m,n}) , \tag{84}$$

$$\frac{\partial \phi_{m,n}}{\partial t} = -\frac{1}{2}\int_{-1}^{1} \frac{1}{1-\mu^2}[imC_m P_{m,n} - D_m \frac{dP_{m,n}}{d\mu}]\, d\mu + \bar{\phi} n(n+1)\, \chi_{m,n} , \tag{85}$$

where

$$E_{m,n} = \frac{1}{2}\int_{-1}^{1} \frac{E_m}{1-\mu^2} P_{m,n}\, d\mu . \tag{86}$$

The integrals are evaluated by the Gaussian quadrature formula as before, but this time $(5M+1)/2$ Gaussian latitudes are required. As before the required number of longitudinal grid points is $3M+1$.

Bourke (1972) compared the efficiency of the transform method to the interaction coefficient method for this model. Figure 2 shows the computer time required per time step for the two methods as a function of the truncation number M. The figure shows clearly that even for $M = 15$ the transform method is an order of magnitude faster than the interaction coefficient method. In fact the interaction coefficient method becomes almost intractable for M much larger than 15. At $M = 15$ there are over 500,000 interaction coefficients.

The system (83)- (85) is very convenient for the application of semi-implicit time differencing. All terms are evaluated explicitly except that $\phi_{m,n}$ in (84) and $\chi_{m,n}$ in (85) are treated implicitly. These two equations are easily solved for $\phi_{m,n}(t+\Delta t)$, and equations (83) and (84)

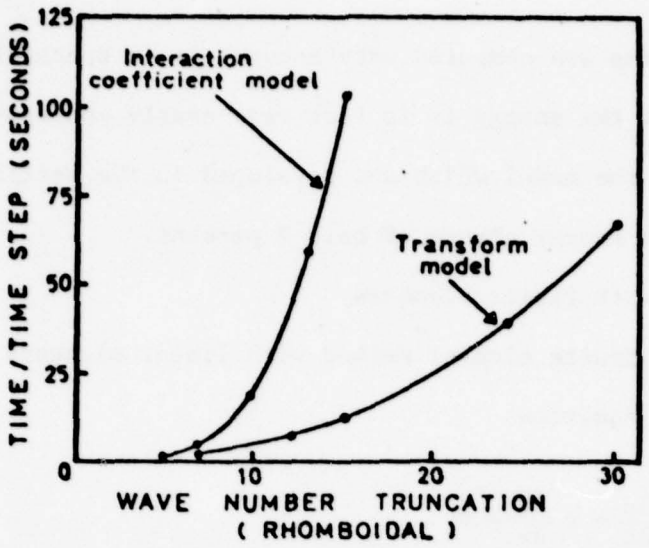

Figure 2. -Computation time per time step (s) as a function of spectral resolution. Integrations of a global spectral model employing a transform method and employing the interaction coefficient method are compared.

can then be solved explicitly. In contrast finite difference models require the solution of a Helmholtz equation for $\phi(t+\Delta t)$, at every time step Thus in spectral primitive equation models a much longer time step can be used with almost the same computational effort per time step.

The introduction of the transform method and semi-implicit differencing have made the spectral primitive equation models competitive with finite difference models for global prediction. The procedures used in this section are easily extended to baroclinic models as has been done by Bourke et al. (1977), Machenhauer and Daley (1972) and Hoskins and Simmons (1975). Comparisons have shown that as good or better forecasts can be made with global spectral models than with finite difference models which use the same amount of computer time (Doron et al. (1974) and Daley, Girard and Simmonds (1976).

It should be pointed out that energy is not exactly conserved in this model even with continuous time variation. This is because the kinetic energy for the shallow water equations is proportional to $\phi\vec{V}\cdot\vec{V}$ which is a cubic energy form, and consequently the analysis of Section 3 does not apply.

However the nonlinear terms are computed very accurately in spectral models and experience shows that the energy is in fact very nearly conserved. Bourke (1972) integrated the model which was developed in the section for 116 days, and obtained an energy change of only 2 percent.

8 Advection Equation with Finite Elements

In this section the finite element method with linear elements will be applied to the advection equation

$$\frac{\partial u}{\partial t} + c \frac{\partial u}{\partial x} = 0 . \tag{87}$$

This equation has been treated extensively with various finite difference schemes. The Galerkin equation is obtained by setting $\mathcal{L} = c \frac{\partial}{\partial x}$ in (22) which gives

$$\sum_{j=1}^{N} \frac{du_j}{dt} \int_a^b \varphi_i \varphi_j dx + c \sum_{j=1}^{N} u_j \int_a^b \varphi_i \frac{\partial \varphi_j}{\partial x} dx = 0 , \quad i=1,\ldots,N. \tag{88}$$

The linear basis functions $\varphi_j(x)$ are defined by (12) and a typical one is shown in Fig. 1. In this application u is periodic so that the basis functions must satisfy $\varphi_o = \varphi_N$ and $\varphi_1 = \varphi_{N+1}$.

The first term in (88) can be evaluated from (17) which is of the same form, and the second term can be computed with the use of (14). The resulting equation with $i = m$ can be written:

$$\frac{1}{6}\left(\frac{du_{m+1}}{dt} + 4\frac{du_m}{dt} + \frac{du_{m-1}}{dt}\right) + c \frac{u_{m+1} - u_{m-1}}{2\Delta x} = 0 . \tag{89}$$

The advection term is the same as is obtained from centered differencing, but the time derivative appears as a weighted average over three points. It

will be seen later that this greatly increases the accuracy of the solution.

Now apply leapfrog time differencing which gives the following equation:

$$\frac{1}{12\Delta t}(u_{m+1,n+1}-u_{m+1,n-1}+4(u_{m,n+1}-u_{m,n-1})+u_{m-1,n+1}-u_{m-1,n-1})+\frac{c}{2\Delta x}(u_{m+1,n}-u_{m-1,n}) = 0 . \tag{90}$$

The stability and phase error can be investigated by substituting $u_{m,n} = A \exp[i(\mu\Delta x m + \alpha\Delta t n)]$ into (90). This yields

$$\sin\alpha\Delta t = -(c\Delta t/\Delta x)(3 \sin\mu\Delta x)/(2 + \cos\mu\Delta x) . \tag{91}$$

The solution is stable (i.e. $(\sin\alpha\Delta t) \leq 1$) if

$$3c\Delta t/\Delta x[\sin\mu\Delta x/(2 + \cos\mu\Delta x)]_{max} \leq 1 .$$

The bracketed term is a maximum when $\mu\Delta x = 120°$, so that the stability condition becomes

$$|c\Delta t/\Delta x| \leq 1/\sqrt{3} . \tag{92}$$

This criterion is considerably more restrictive than the CFL condition which arises from the leapfrog finite difference scheme. However it will be shown that (90) gives even better phase speed than the fourth-order leapfrog scheme for which the computational stability criterion is $|c\Delta t/\Delta x| \leq 0.73$ Thus it is not unreasonable that the leapfrog finite element scheme would have a more restrictive computational stability criteria.

The finite element formula with leapfrog time differencing is actually implicit, since the new value $u_{m,n+1}$ cannot be obtained explicitly from the earlier time values. Thus it seems reasonable to use a fully implicit form which does not have the timestep restriction (92). Consider the following time difference approximation to (89):

$$\frac{1}{6\Delta t}(u_{m+1,n+1}-u_{m+1,n} + 4(u_{m,n+1}-u_{m,n}) + u_{m-1,n+1}-u_{m-1,n})$$

$$+ \frac{c}{4\Delta x}(u_{m+1,n+1}-u_{m-1,n+1} + u_{m+1,n}-u_{m-1,n}) = 0 . \qquad (93)$$

This fully implicit scheme can be shown to be neutral for all timesteps, and it should require about the same effort per time step as (90). For this reason implicit time differencing schemes are often desirable when finite elements are used.

The phase speed for the leapfrog scheme is given by

$$c_F = -\alpha/\mu = \frac{1}{\mu\Delta t}\arcsin\left(\frac{c\Delta t}{\Delta x}\frac{3\sin\mu\Delta x}{2+\cos\mu\Delta x}\right) . \qquad (94)$$

If $\Delta t/\Delta x$ and μ are fixed, this expression approaches $\hat{c}$ as $\Delta t \to 0$, which shows that the solution converges. If Δt is small in comparison to $\Delta x/c$, this formula reduces to

$$c_F = \frac{c}{\mu\Delta x}\frac{3\sin\mu\Delta x}{2+\cos\mu\Delta x} = \frac{c}{\mu\Delta x}\frac{\sin\mu\Delta x}{[1-2/3\ \sin^2(\mu\Delta x/2)]} . \qquad (95)$$

Table 1 contains c/c_F from ((95) for typical values of L .

L	$2\Delta x$	$3\Delta x$	$4\Delta x$	$6\Delta x$
FEM	0	0.83	0.96	0.99
4th order	0	0.61	0.85	0.96

Table 1: c/c_F for the FEM solution and for 4th order space differenced scheme for various wavelengths L.

The table also includes the ratio for the fourth order scheme from the limit for small Δt . The finite element formula (95) can be expanded

in $\mu\Delta x$ which leads to an error that is of order $(\mu\Delta x)^4$. Table 1 shows that although the linear finite element equation and the fourth order finite difference equation have the same order of truncation error, the finite element equation is much more accurate. At $L = 3\Delta x$ the finite element solution gives only 17% error in phase speed, while the fourth-order finite difference gives 39%. However for $L = 2\Delta x$, $c_F = 0$, which indicates that the finite element computational group velocity is very large for this wavelength. This can be shown by differentiating as follows:

$$c = \frac{d(\mu c_F)}{d\mu} = \frac{[2\cos\mu\Delta x + 1]}{(\cos\mu\Delta x + 2)^2} . \qquad (96)$$

When $L = 2\Delta x$ ($\mu\Delta x = \pi$) this formula gives $G = -3c$ which is much larger than the $-(5/3)c$ that occurs with fourth-order differencing. This suggests that small scale noise will propagate very rapidly in finite element models. This tendency toward noisiness has been observed in various finite element models. The degree of accuracy indicated above for the finite element model has been verified by Cullen (1973) in a two-dimensional advective problem. It should be noted that although the FEM gives a solution for all values of x in the range considered, the high accuracy is only obtained at the nodal points since the fields are assumed to be linear between nodal points. In the next section the method will be applied to the barotropic vorticity equation.

9. Barotropic Vorticity Equation with Finite Elements

In this section the finite element method will be applied to the non-linear barotropic vorticity equation in a two-dimensional domain. The basis functions will be linear functions on triangular elements. The barotropic vorticity equation can be written

$$\frac{\partial \eta}{\partial t} = -\vec{k} \times \nabla\psi \cdot \nabla\eta \ , \qquad (97)$$

where

$$\eta = f(y) + \nabla^2\psi \ , \qquad (98)$$

is the absolute vorticity.

Following Fix (1975) both ψ and η are expanded in terms of the basis functions $\varphi_j(x,y)$ as given below:

$$\psi(x,y,t) = \sum_{j=1}^{N} \psi_j(t)\, \varphi_j(x,y) \ , \qquad (99)$$

$$\eta(x,y,t) = \sum_{j=1}^{N} \eta_j(t)\, \varphi_j(x,y) \ . \qquad (100)$$

When the Galerkin method is applied to (98) the following is obtained:

$$\sum_{j=1}^{N} \dot{\psi}_j(t) \iint \varphi_i \nabla^2 \varphi_j \, dA = -\iint \varphi_i(x,y) f(y) dA + \sum_{j=1}^{N} \eta_j(t) \iint \varphi_i(x,y)\, \varphi_j(x,y) dA \ ,$$

for $i=1,..,N$. Since linear basis functions will be used it is necessary to integrate the left hand side by parts, which gives:

$$\sum_{j=1}^{N} \dot{\psi}_j \iint \nabla\varphi_i \cdot \nabla\varphi_j dA = \iint \varphi_i f(y) dA - \sum_{j=1}^{N} \dot{\eta}_j \iint \varphi_i \varphi_j dA \ , \qquad (101)$$

for $i=1,2,\ldots,N$.

The boundary terms which arise from the integration by parts were set to zero, by assuming that either ψ is periodic in space or that there is no flow normal to the boundaries(i.e., $\vec{k}x\nabla\psi\cdot\vec{n} = 0$, where $\vec{n}$ is a unit vector normal to the boundary). Now apply the Galerkin method to the vorticity equation (97), which leads to the following form:

$$\sum_{j=1}^{N} \frac{d\eta_j}{dt}\iint \varphi_i\varphi_j dA = -\sum_{j=1}^{N}\sum_{k=1}^{N} \psi_j\eta_k \iint \varphi_i \vec{k} \times \nabla\varphi_j \cdot \nabla\varphi_k dA , \qquad (102)$$

for $i=1,\ldots,N$. This equation is of the same form that was obtained with the spectral model, but the nonlinear term requires much less effort because the only φ's which interact are those which are physically adjacent.

The equations (101) and (102) conserve both mean square vorticity (enstrophy) and kinetic energy. The enstrophy conservation can be shown by multiplying (102) by η_i and summing over i. When the sumations are taken under the integrals, the form (26) is found. Since the integral of $\eta\vec{k} \times \nabla\psi\cdot\nabla\eta$ vanishes, the conservation of $\eta^2/2$ follows directly. The kinetic energy change can be examined by first differentiating (101) and substituting the result into (102) which gives:

$$-\sum_{j=1}^{N} \frac{d\psi_j}{dt}\iint \nabla\varphi_i\cdot\nabla\varphi_j dA = -\sum_{j=1}^{N}\sum_{k=1}^{N} \psi_j\eta_k \iint \varphi_i \vec{k} \times \nabla\varphi_j \cdot \nabla\varphi_k dA , \qquad (103)$$

for $i=1,2,\ldots,N$. Multiply this equation by $-\psi_i$ and sum over i. The resulting equation is again of the same form as (26) and the left hand side is the derivative of the total kinetic energy. Since the integral of $\psi\vec{k} \times \nabla\psi\cdot\nabla\eta$ is zero, the energy is conserved. These results are not dependent on the particular basis functions which are employed.

The systems of equations (101) and (102) can be written in matrix forms which are more convenient for solution. Let $\vec{\psi}$ and $\vec{\eta}$ be column

vectors of the values of ψ_i and η_i, respectively. Then (101) takes the form:

$$K\vec{\psi} = \vec{Q} , \qquad (104)$$

where the elements of the matrix K are

$$K_{ij} = \iint \nabla\varphi_j \cdot \nabla\varphi_i dA , \qquad (105)$$

and $\vec{Q}$ is a column vector of the right hand side of (101). Similarly, system (102) becomes

$$M \frac{d\vec{\eta}}{dt} = \vec{J} , \qquad (106)$$

where the elements of M are

$$M_{ij} = \iint \varphi_i \varphi_j \, dA , \qquad (107)$$

and $\vec{J}$ is a column vector of the right hand side of (102).

The solution procedure will be illustrated for the case where leapfrog time differencing is used in (105) which leads to the equation:

$$M\Delta\vec{\eta} = 2\Delta t \, \vec{J}_n , \qquad (108)$$

where $\Delta\vec{\eta} = \vec{\eta}_{n+1} - \vec{\eta}_{n-1}$. The matrices K and M are computed initially and stored for later use. The equations can be integrated beginning with $\psi_{j,n}$, $\eta_{j,n-1}$ and $\eta_{j,n}$. The right hand side of (108) can be computed from $\psi_{j,n}$ and $\eta_{j,n}$, and that equation can then be solved for Δn_j. This increment can be added to $\eta_{j,n-1}$ to obtain $\eta_{j,n+1}$. With these values the right hand side of (104) can be computed, and (104) can be solved for $\psi_{j,n+1}$, and the process can be continued. In this procedure it is necessary to invert the matrices K and M during each time step. These matrices are very sparse since only adjacent elements interact. In some cases direct

methods can be used, but iterative methods are much more flexible.

Cullen (1973) has shown that the two dimensional advective stability criterion for linear elements is

$$\frac{|c|\Delta t}{d} \leq 1/\sqrt{6} , \tag{109}$$

where d is the distance between nodal points. This is consistent with the one-dimensional result (92), because the step from one to two dimensions is usually achieved by replacing the grid size with $d/\sqrt{2}$. In this application $|c|$ would correspond to the maximum velocity in the domain. Since the condition (108) is rather restrictive for Δt and since two matrices must be inverted per time step it may be worth while to use a fully implicit form similar to (93).

The natural generalization of the tent function in one dimension to two dimensions is a basis function which is composed of triangular elements. On each triangle the function varies linearly from 0 at two vertices to 1 at the third which is the nodal point for the basis function. Figure 3 shows how a typical basis function φ_j is constructed on a rectangular grid of nodal points. This function is the sum of the six plane surfaces that are associated with each triangle. The basis functions can be equally well constructed when the nodal points are irregularly located, and it is not necessary to have six triangular elements in the construction.

The elements in the matrix equations (104) and (106) are obtained by evaluating the integrals in equations (101) and (106). These integrals can be reduced to a series of integrals over triangles such as are shown in Figure 3. Within each triangle any point is affected by only the three basis functions which have nodal points at the three vertices of the triangle. Zienkiewicz (1971) and Desai and Abel (1972) describe a convenient procedure

for evaluating the integrals over each triangle. This involves introducing triangular coordinates which vary linearly across each triangle in the same manner as the basis functions. The integrals can then be evaluated quite generally.

A rigorous mathematical analysis of the finite element method is given in the book by Strang and Fix (1973). The stability and convergence of the method are discussed in considerable detail. Most finite element applications are based on a variational formulation rather than the Galerkin approach which has been used here, although the Galerkin method is most appropriate when time dependence is included. Pinder and Gray (1977) developed the finite element metood with the Galerkin approach, and gave applications in hydrology which has similar equations to those which occur in numerical weather prediction.

The finite element method has been applied to atmospheric prediction with the primitive equations in shallow water form. Cullen (1974) and Hinsman (1975)

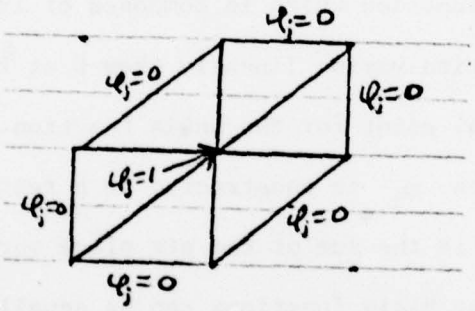

Fig. 3. Construction of the basis function φ_j on a rectangular array of nodal points.

carried out global forecasts with these equations using linear basis functions on triangles as discussed in this section. The elements were efficiently arranged so that the area of each element was almost the same over different parts of the globe. Most global finite difference models have a large variation in grid size between the equator and the pole, and consequently are not very efficient.

Staniforth and Mitchell (1977) reformulated the shallow water equations in terms of the vorticity and divergence as was done in section 6.6 for the spectral model. In this form semi-implicit time differencing can be applied easily, which allows a much larger time step. This is very important since the finite element method generally requires more computer time per time step. Staniforth and Mitchell also found very little noise generation in their forecasts, whereas many finite element primitive equation models tend to generate small scale noise if no smoothing is used [Cullen (1976)].

The finite element method when applied to meteorological equations gives very accurate phase propagation and also handles nonlinearities very well. The main drawback to the use of the method is the requirement that an equation solver must be applied to invert a large matrix at every time step for every variable. The development of flexible exact solvers for these matrices is of great importance. The finite element method can easily be applied to variable resolution problems, but some finite element models do tend to produce noise probably as a result of the large spurious group velocity for the shortest wave. However, the formulation of Staniforth and Mitchell (1977) seems to reduce this problem considerably. Schoenstadt (1978) has shown that noise is generated in finite element models where all variables are carried at the same models points. When the variables are staggered at different model points or when the vorticity and divergence equation are used this problem can be avoided. The general procedure used by Staniforth and Mitchell (1977) appears to be superior because semi-implicit differencing can be easily implimented, and the forecasts are not noisy.

References

Baer, F. and G. W. Platzman, 1961: The extended numerical integration of a simple barotropic model. J. Meteor., 18, 393-401.

Bourke, W., 1972: An efficient, one-level, primitive-equation spectral model. Mon. Wea. Rev., 100, 683-689.

Bourke, W., B. McAvaney, K. Pari and R. Thurling, 1977: Global modeling of atmospheric flow by spectral methods. Methods in Computational Physics, 17, 267-324.

Cooley, J. W. and J. W. Tukey, 1965: An algorithm for the machine computation of complex Fourier series. Math. Comp., 19, 297-301.

Cullen, M. J. P., 1973: A simple finite element method for meteorological problems. J. Inst. Math. Applics., 11, 15-31.

_____, 1974: Integration of the primitive equations on a sphere using the finite element method. Quart. J. R. Met. Soc., 100, 555-562.

_____, 1976: On the use of artificial smoothing in Galerkin and finite difference solutions of the primitive equations. Quart. J. R. Met. Soc., 102, 77-93.

Daley, R., C. Girard, J. Henderson and I. Simmonds, 1976: Short-term forecasting with a multi-level spectral primitive equation model. Atmosphere, 14, 98- .

Desai, C. S. and J. Abel, 1972: Introduction to the Finite Element Method. Van Nostrand Reinhold, New York.

Doron, E., A. Hollingsworth, B. J. Hoskins, and A. Simmons, 1974: A comparison of grid-point and spectral methods in a meteorological problem. Quart. J. R. Met. Soc., 100, 371-383.

Eliasen, E., B. Machenhauer, and E. Rasmussen, 1970: On a Numerical Method for Integration of the Hydrodynamical Equations with a Spectral Representation of the Horizontal Fields, Rep. No. 2, Institut for Teoretisk Meteorologi, Kobenhavns Universitet, Denmark, 35 pp.

Fix, G., 1975: Finite element models for ocean circulation problems. Siam J. Appl. Math., 29(3), 371-387.

Hinsman, D. E., 1975: Application of a Finite Element Method to the Barotropic Primitive Equations. M.S. Thesis, Naval Postgraduate School, Monterey, California, 116 pp.

Hoskins, B. J. and A. J. Simmons, 1975: A multi-layer spectral model and the semi-implicit method. Quart. J. R. Met. Soc., 101, 637-655.

Lorenz, E. N., 1960: Maximum simplification of the dynamic equations. Tellus, 12, 243-254.

Machenhauer, B., and R. Daley, 1972: A Baroclinic Primitive Equation Model with a Spectral Representation in Three Dimensions. Rep. No. 4, Institut for Teoretisk Meteorologi, Kobenhavns Universitet, Denmark,

_____, and E. Rasmussen, 1972: On the Integration of the Spectral Hydrodynamical Equation by a Transform Method. Rep. No. 3, Institut for Teoretisk Meteorologi, Kobenhavns Universitet, Denmark, 44 pp.

Orszag, S. A., 1969: Numerical methods for the simulation of turbulence. Phys. Fluids, Suppl. II, 12, 250-257.

_____, 1970: Transform method for the calculation of vector-coupled sums: Application to the spectral form of the vorticity equation. J. Atmos. Sci., 27, 890-895.

_____, 1971: Numerical simulation of incompressible flows within simple boundaries: Galerkin, spectral representations. Studies in Appl. Math., 50, 293-327.

Platzman, G. W., 1960: The spectral form of the vorticity equation. J. Meteor., 17, 635-644.

Pinder, G. F. and W. G. Gray, 1977: Finite Element Simulation in Surface and Subsurface Hydrology. Academic Press, New York, 295 pp.

Schoenstadt, A. L., 1978: A Transfer Function Analysis of Numerical Schemes Used to Simulate Geostrophic Adjustment. Naval Postgraduate School Report, NPS-53-79-001, 44 pp.

Silberman, I. S., 1954: Planetary waves in the atmosphere. J. Meteor., 11, 27-34.

Staniforth, A. N., and H. L. Mitchell, 1977: A semi-implicit finite-element barotropic model. Mon. Wea. Rev., 105, 154-169.

Strang, G. W. and G. J. Fix, 1973: An Analysis of the Finite Element Method. Prentice-Hall, Englewood Cliffs, N.J., 306 pp.

Zienkiewicz, O. C., 1971: The Finite Element Method in Engineering Science. McGraw Hill,

DISTRIBUTION LIST

		No. Copies
1.	Defense Documentation Center Cameron Station Alexandria, Virginia 22314	2
2.	Library, Code 0142 Naval Postgraduate School Monterey, California 93940	2
3.	Dr. R. T. Williams, Code 63Wu Department of Meteorology Naval Postgraduate School Monterey, California 93940	10
4.	Commander Naval Oceanography Command National Space Technology Laboratories Bay St. Louis, Mississippi 39520	1
5.	Officer in Charge Naval Environmental Prediction Research Facility Monterey, California 93940	10
6.	Dean of Research, Code 012 Naval Postgraduate School Monterey, California 93940	2
7.	Commanding Officer Fleet Numerical Weather Central Monterey, California 93940	10
8.	Naval Oceanographic Office Library, Code 3330 Washington, D. C. 20373	1
9.	Air Force Geophysics Laboratory Exchange Librarian Sulls Stop 29 Hanscom AFB Bedford, Massachusetts 01730	1
10.	Commander, Air Weather Service Military Airlift Command United States Air Force Scott Air Force Base, Illinois 62226	1
11.	Dr. A. Arakawa Department of Meteorology University of California Los Angeles, California 90024	1

12. Captain John L. Hayes 1
Air Force Global Weather Central
PSC #2, Box 7141
Offutt AFB, Nebraska 68113

13. Atmospheric Sciences Library 1
National Oceanic and Atmospheric Administration
Silver Spring, Maryland 20910

14. Dr. F. P. Bretherton 1
National Center for Atmospheric Research
P. O. Box 3000
Boulder, Colorado 80303

15. Dr. John Brown 1
National Meteorological Center/NOAA
World Weather Building
Washington, D. C. 20233

16. Dr. C.-P. Chang, Code 63Cp 1
Department of Meteorology
Naval Postgraduate School
Monterey, California 93940

17. Prof. J. G. Charney 1
54-1424
Massachusetts Institute of Technology
Cambridge, Massachusetts 02139

18. Dr. C. Comstock, Code 53Zk 1
Department of Mathematics
Naval Postgraduate School
Monterey, California 93940

19. Dr. M. J. P. Cullen 1
Meteorological Office
Bracknell, Berks
United Kingdom

20. Dr. R. L. Elsberry, Code 63Es 1
Department of Meteorology
Naval Postgraduate School
Monterey, California 93940

21. Prof. F. D. Faulkner, Code 53Fa 1
Naval Postgraduate School
Monterey, California 93940

22. Dr. W. L. Gates 1
Department of Meteorology
Oregon State University
Corvallis, Oregon 97331

23. Dr. Earl Gossard
Wave Propagation Laboratory
NOAA/ERL
Boulder, Colorado 80302 — 1

24. Dr. G. J. Haltiner, Code 63Ha
Chairman, Department of Meteorology
Naval Postgraduate School
Monterey, California 93940 — 1

25. Dr. R. L. Haney, Code 63Hy
Department of Meteorology
Naval Postgraduate School
Monterey, California 93940 — 1

26. Lieutenant D. Hinsman
Fleet Numerical Weather Central
Monterey, California 93940 — 1

27. Dr. J. Holton
Department of Atmospheric Sciences
University of Washington
Seattle, Washington 98105 — 1

28. Dr. B. J. Hoskins
Department of Geophysics
University of Reading
Reading, United Kingdom — 1

29. Dr. D. Houghton
Department of Meteorology
University of Wisconsin
Madison, Wisconsin 53706 — 1

30. Dr. S. K. Kao
Department of Meteorology
University of Utah
Salt Lake City, Utah 84112 — 1

31. Dr. A. Kasahara
National Center for Atmospheric Research
P. O. Box 3000
Boulder, Colorado 80303 — 1

32. Cdr. W. R. Lambertson
Fleet Weather Facility Suitland
Navy Department
Washington, D. C. 20373 — 1

33. Dr. C. E. Leith
National Center for Atmospheric Research
P. O. Box 3000
Boulder, Colorado 80303 — 1

34. Dr. J. M. Lewis — 1
Laboratory for Atmospheric Research
University of Illinois
Urbana, Illinois 61801

35. Dr. E. N. Lorenz — 1
Department of Meteorology
Massachusetts Institute of Technology
Cambridge, Massachusetts 02139

36. Lieutenant Olaf M. Lubeck — 1
COMNAVMARIANAS, Box 12
FPO San Francisco 96630

37. Dr. R. Madala — 1
Code 7750
Naval Research Laboratories
Washington, D. C. 20390

38. Dr. J. D. Mahlman — 1
Geophysical Fluid Dynamics Laboratory
Princeton University
Princeton, New Jersey 08540

39. Meteorology Library, Code 63 — 1
Naval Postgraduate School
Monterey, California 93940

40. National Center for Atmospheric Research — 1
Box 1470
Boulder, Colorado 80302

41. Director, Naval Research Laboratory — 1
ATTN: Technical Services Information Center
Washington, D. C. 20390

42. Department of Oceanography, Code 68 — 1
Naval Postgraduate School
Monterey, California 93940

43. Office of Naval Research — 1
Department of the Navy
Washington, D. C. 20360

44. Dr. T. Ogura — 1
Laboratory for Atmospheric Research
University of Illinois
Urbana, Illinois 61801

45. Prof. K. Ooyama — 1
National Center for Atmospheric Research
P. O. Box 3000
Boulder, Colorado 80303

46. Dr. I. Orlanski — 1
Geophysical Fluid Dynamics Laboratory
Princeton University
Princeton, New Jersey 08540

47. Prof. N. A. Phillips — 1
National Meteorological Center/NOAA
World Weather Building
Washington, D. C. 20233

48. Dr. S. Piacsek — 1
NORDA 320
NSTL Station, Mississippi 39529

49. Dr. T. Rosmond — 3
Naval Environmental Prediction Research Facility
Monterey, California 93940

50. Dr. Y. Sasaki — 1
Department of Meteorology
University of Oklahoma
Norman, Oklahoma 73069

51. Prof. A. L. Schoenstadt, Code 53Zh — 1
Naval Postgraduate School
Monterey, California 93940

52. Dr. Fred Shuman, Director — 1
National Meteorological Center
World Weather Building
Washington, D. C. 20233

53. Dr. J. Smagorinsky, Director — 1
Geophysical Fluid Dynamics Laboratory
Princeton University
Princeton, New Jersey 08540

54. Dr. R. Somerville — 1
National Center for Atmospheric Research
P. O. Box 3000
Boulder, Colorado 80303

55. Dr. Andrew Staniforth — 1
Recherche en Prevision Numerique
West Isle Office Tower, 5 ieme etage
2121 route Trans-Canada
Dorval, Quebec H9P1J3
Canada

56. Dr. D. Williamson — 1
National Center for Atmospheric Research
P. O. Box 3000
Boulder, Colorado 80303

57. Dr. M. G. Wurtele
Department of Meteorology
University of California
Los Angeles, California 90024 1

58. Dr. J. Young
Department of Meteorology
University of Wisconsin
Madison, Wisconsin 53706 1